TISSUE ENGINEERING: Part A
Volume 25, Numbers 17 and 18, 2019

DOI: 10.1089/ten.tea.2018.0239

termis
Tissue Engineering
& Regenerative Medicine
International Society

ORIGINAL ARTICLE

Development of Intestinal Scaffolds that Mimic Native Mammalian Intestinal Tissue

Mitchell R. Ladd, MD, PhD,[1] Cait M. Costello, PhD,[2] Carolyn Gosztyla, MD,[3] Adam D. Werts, DVM, PhD,[1] Blake Johnson, BS,[1] William B. Fulton, MS,[1] Laura Y. Martin, MD,[1] Elizabeth J. Redfield,[2] Bryan Crawford, MS,[4] Rohan Panaparambil,[5] Chhinder P. Sodhi, PhD,[1] John C. March, PhD,[2] and David J. Hackam, MD, PhD[1]

The goal of this study was to develop a scaffold for the generation of an artificial intestine that specifically mimics the architecture and biomechanical properties of the native small intestine, and to evaluate the scaffold *in vitro* and *in vivo*. Scaffolds mimicking the microarchitecture of native intestine were fabricated from poly(glycerol sebacate) (PGS) with a thickness of 647 μm (±241 μm) and villus height of 340 μm (±29.5 μm). The scaffolds showed excellent biological properties, as 71.4% (±7.2%) and 58.7% (±12.7%) mass remained after 5 weeks of *in vitro* exposure to control and digestive media, respectively. Tensile properties of the scaffolds approached those of native porcine intestine and scaffolds maintained their mechanical properties over 6 weeks based on rheometer measurements. Scaffolds accommodated intestinal epithelial stem cells and demonstrated maintenance of size and microarchitecture after 12 weeks of omental implantation in mice. There was an expected amount of inflammation, but less tissue infiltration and tissue formation than anticipated. In conclusion, we developed novel scaffolds using PGS that mimic the microarchitecture and mechanical properties of native intestine with promise for use in artificial intestine for individuals with short bowel syndrome.

Graphical Abstract

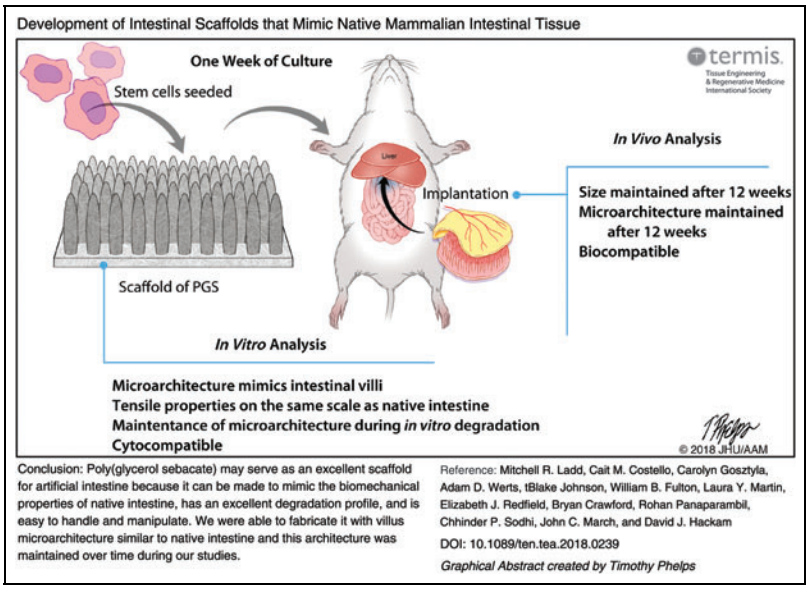

Color images are available online.

[1]Department of Surgery, Johns Hopkins School of Medicine, Baltimore, Maryland.
[2]Department of Biological and Environmental Engineering, Cornell University, Ithaca, New York.
[3]Department of Surgery, Walter Reed National Military Medical Center, Bethesda, Maryland.
Departments of [4]Materials Science and Engineering and [5]Biomedical Engineering, Johns Hopkins University, Baltimore, Maryland.

Keywords: intestinal tissue engineering, artificial intestine, functional tissue engineering with intestinal scaffolds, poly(glycerol sebacate) scaffold biomechanics, biodegradable polymers, short bowel syndrome

Impact Statement

This study is significant because it demonstrates an attempt to design a scaffold specifically for small intestine using a novel fabrication method, resulting in an architecture that resembles intestinal villi. In addition, we use the versatile polymer poly(glycerol sebacate) (PGS) for artificial intestine, which has tunable mechanical and degradation properties that can be harnessed for further fine-tuning of scaffold design. Moreover, the utilization of PGS allows for future development of growth factor and drug delivery from the scaffolds to promote artificial intestine formation.

Introduction

SHORT BOWEL SYNDROME is a highly morbid and costly disease with high mortality, which can affect infants and children, and represents a serious complication of necrotizing enterocolitis, gastroschisis, or intestinal volvulus.[1–4] The primary treatment modality for short bowel syndrome is parenteral nutrition, allowing time to encourage the native intestine to adapt and attain enteral autonomy.[2] Importantly, the long-term use of parenteral nutrition is associated with severe complications, including liver failure, sepsis, and death,[2,3,5–8] and the intestine often fails to adapt due to inadequate starting length.

Surgical options exist to improve intestinal length, but they are typically used as a last resort and when the intestine is severely dilated.[6,7,9,10] When all else fails, the final treatment approach is small bowel transplantation, which, despite many advances, remains highly morbid and requires life-long immunosuppression.[11] Based on the lack of effective options for the treatment of short bowel syndrome, there is a pressing need for the development of an engineered replacement option, namely the development of an artificial intestine.[6,7,12]

Several investigators have worked toward the development of an artificial intestine,[13–17] and have used poly(glycolic acid), polyanhydrides, and polyorthoester. It is noteworthy that the materials tested have not changed since that time, such that the majority of groups continue to use variations of these polymers.[15–18] These materials were primarily chosen because they are readily available, off-the-shelf, and are Food and Drug Administration approved, biodegradable materials. Since the initial use of these materials, a body of literature has emerged demonstrating the importance of designing scaffolds that recapitulate the properties of the tissue one wishes to regenerate.[19–21] The study of such materials is considered a subfield of tissue engineering called ''functional tissue engineering.''[20] In particular, mechanical properties of scaffolds are known to be important, and need to address the structural integrity of the tissue as well as the interplay between cells and materials, that is, the mechanobiology.[19–21] Despite this, the successful design of a biomaterial scaffold for use in intestinal tissue engineering that recapitulates the biomechanical, structural, and functional properties of the native gut remains an unmet need in the fields of tissue engineering and organ replacement science.[7,23]

The goal of this study was to develop a scaffold designed specifically for use in intestinal tissue engineering. In particular, we sought to develop a scaffold that mimicked the microarchitecture of native intestine (i.e., contained villus structures) and had similar mechanical properties to native intestine. We hypothesized that such a scaffold would be capable of supporting intestinal stem cells and would recruit and form intestinal tissue *in vivo*. We chose poly(glycerol sebacate) (PGS) for this purpose because it is a well-studied biomaterial that undergoes surface degradation, has tunable degradation and mechanical properties depending on the amount of crosslinking performed, and is known to have excellent biocompatibility. We anticipated that PGS would be easier to fine-tune because it can be fine-tuned by varying the amount of crosslinking alone, in contrast to other materials, such as poly-lactic-co-glycolic acid (PLGA), which require changing the relative ratios of polyglycolic acid and polylactic acid. Moreover, we have used PLGA in the past and found these scaffolds to be brittle and much stiffer than native intestine.[17,23]

Methods

Experimental animals

All animal studies were approved by the Institutional Animal Care and Use Committee at the Johns Hopkins University under the protocol number M017M304. C57bl/6 (wild type) and Rosa26$^{CMV\text{-}cre\text{-}EGFP}$ mice (which express the fluorescent marker green fluorescent protein [GFP] in all cells) were used for cell isolation. C57bl/6 mice were used for surgery. Discarded, 21-day-old male pig intestine was obtained from deceased pigs that were used in terminal experiments (protocol number SW14M223).

Cell media and reagents

Incomplete chelating solution (ICS) for intestinal stem cell isolation (5×) consisted of 1.97 g of anhydrous Na_2HPO_4, 2.7 g KH_2PO_4, 14 g NaCl, 0.3 g KCl, 37.5 g sucrose, and 25 g D-sorbitol in 0.5 mL of Millipore deionized water as described.[24–27] This solution was filter sterilized and kept at 4°C until use and is stable for several months. 1× complete chelating solution (CCS) was prepared by combining 100 mL of 5×ICS with 40 mg of dithiothreitol and then bringing the entire solution up to 500 mL with Millipore deionized water. CCS was kept at 4°C for a maximum of 7 days before use. Matrigel with phenol red (Fisher Scientific; 354234) was used for maintaining intestinal stem cells in culture and for experiments that did not require microscopy. Matrigel without phenol red (Fisher Scientific; 356237) was used for experiments that were to undergo microscopy. Cell media growth factor negative (CMGF–) media consisted of Advanced Dulbecco's modified Eagle

medium (DMEM, 11320-082; Invitrogen), 2 mM Glutamax (Invitrogen; 35050-061), 10 mM HEPES buffer (Sigma; 83264), 1 × N_2 supplement (Invitrogen; 17502-048), 1 × B-27 supplement minus Vitamin A (Invitrogen; 12587-010), and 1 × primocin (Invitrogen; ant-pm-2) as described.[24–27] CMGF positive (CMGF+) media consisted of CMGF– media plus 10 nM gastrin, 1 mM *N*-acetylcysteine, Wnt3A (from conditioned medium), R-spondin 1 (from conditioned medium), 50 ng/mL epidermal growth factor (EGF), 100 ng/mL Noggin, 500 nM A83-01, and 10 μM SB202190 as previously reported.[27] Mouse minimal media consisted of CMGF–, 100 ng/mL Wnt3A, 1000 ng/mL R-spondin 1, 100 ng/mL Noggin, 1 × B-27 supplement, 1 mM *N*-acetylcysteine, 50 ng/mL EGF, and 1 × primocin. Y-27632 (Sigma Aldrich; Y0503) was used in CMGF+ or mouse minimal media after passaging as described.[24–27] Stock 1000 × Y-27632 was made at a concentration of 10 mM in dimethylsulfoxide. This was then diluted to 10 μM (or 1 ×) concentration in cell media before use.

Scaffold fabrication

Scaffolds were synthesized from poly(glycerol sebacate) (PGS, 900210; Sigma-Aldrich) into three-dimensional structures that mimic the native intestine as we have previously reported.[23,28,29] To do so, in brief, laser ablation (Versalaser; Universal Laser Systems, Scottsdale, AZ) was used to create a template array of 500 μm deep, high aspect-ratio holes on a polymethyl-methacrylate (PMMA) template. Polydimethylsiloxane (PDMS; Dow Corning, MI) was used to fabricate ~8 cm × 4 cm replicas of the final bioscaffold with a full villus array as described previously.[30] Molten agarose (3% in water; Sigma, St. Louis, MO) was then poured over the PDMS scaffolds and cooled at room temperature to form hydrogel replicas of the initial PMMA molds. Scaffolds were then fabricated using a modified version of a porogen leaching/thermally induced phase separation technique.[23] The polymer solution was then poured into the mold and processed according to previously published methods to create the final porous scaffold.[23] Thirty percent PGS solution in chloroform was used. The scaffolds were made in a layered manner with the solution used for the top and villus portion of the scaffold mixed with preminced sodium bicarbonate powder (400 mg/mL) with particles roughly 10 μm in diameter as the porogen. This solution was then poured in the mold. Various amounts of the crosslinker 4,4′-methylenebis(phenyl isocyanate) (MDI, 256439; Sigma-Aldrich) were dissolved in the PGS solution for the villus layer (ranging from 2% to 6%) before adding the porogen to optimize the stiffness and degradation of the villus portion of the scaffold. The base portion of the scaffold was made in a similar manner, except that larger sodium bicarbonate particles were used to increase the base pore size (~100–150 μm) and only a 2% MDI concentration was used for the base. The base layer was added before the villus layer completely setting such that at the end of fabrication, the scaffolds were a continuous material.

Porosity measurements

Scaffold porosity was measured by ethanol displacement.[31] A pycnometer was filled with ethanol and weighed as W_1. Scaffolds with weight W_S were immersed into the bottle and submerged in the ethanol. The pycnometer was refilled with ethanol and weighed as W_2. The scaffold saturated with ethanol was removed from the pycnometer and then the pycnometer was weighed as W_3. The following calculations were used to determine porosity:

$$\text{Volume of the scaffold: } V_S = (W_1 - W_2 + W_S)/\rho$$

$$\text{Total volume of the pores: } V_p = (W_2 - W_3 - W_S)/\rho$$

$$\text{Scaffold porosity: } \varepsilon = V_p/(V_p + V_S) = (W_2 - W_3 - W_S)/(W_1 - W_3)$$

Scanning electron microscopy characterization of scaffold

For scanning electron microscopy (SEM), all samples were processed as previously described.[32] In brief, samples fixed were fixed in 5% glutaraldehyde in 3 mM $MgCl_2$ and 0.1 M sodium cacodylate buffer, pH 7.2, overnight at 4°C. Afterward, they were rinsed thrice for 15 min each in 3 mM $MgCl_2$ and 3% sucrose in 0.1 M sodium cacodylate buffer. Next, specimens were fixed in 1% osmium tetroxide in 3 mM $MgCl_2$ in 0.1 M sodium cacodylate buffer for 1 h on ice. After osmium tetroxide fixing, the specimens were rinsed twice in deionized water for 5 min each before undergoing dehydration in graded series of ethanol. The final three changes in the dehydration were a 1:1 ratio of 100% ethanol and hexamethyldisilazane, and the samples were placed in a dessicator to dry. Once dry, the samples were mounted on stands with carbon tape and then sputter-coated with gold-palladium before imaging.

Cell isolation and culture

Caco-2 cell (ATCC, Manassa, VA) passage 25–35 was maintained and expanded in culture flasks in DMEM with 10% fetal bovine serum (FBS) and 1 × antibiotic/antimycotic. The cells were kept in a humidified 37°C incubator with 5% CO_2. Media were changed every 2–3 days and with regular passage 1–2 times a week, and cultured for use in the MTT assay.

Intestinal epithelial stem cells (enteroids) were isolated from juvenile (~P7–P18) C57bl/6 mice or 9-day-old $Rosa26^{CMV\text{-}cre\text{-}EGFP}$ mice and were isolated according to the protocols of Sato *et al.* and Fujii *et al.*[26,27] All tubes and pipettes were coated in FBS to prevent intestinal stem cells from binding to the plastic and decreasing the yield.

Mice were euthanized and the entire intestine was removed. The last 1–3 cm of the ileum was removed for crypt isolation. Intestinal specimens were placed in 10 mL of 1 × complete chelating solution in a 10-cm petri dish and minced into small (2–4 mm) pieces using scissors. Then, the tissue and complete chelating solution were pipetted into a 15-mL conical tube and vigorously triturated (while avoiding air bubbles) 8–10 times to help remove debris and intestinal succus. Afterward, the tissue fragments were allowed to settle by gravity to the bottom of the conical tube, while in ice (for about 1 min). The supernatant was then removed and 10 mL of fresh complete chelating solution was added to the tube, and the

washing procedure repeated. Washing was performed 4–5 times until the supernatant becomes clear. After the last wash, the supernatant was removed leaving about 3 mL of complete chelating solution behind. Next, the entire volume was transferred to one well of a six-well cell culture plate and 200–400 μL of 0.5 M ethylenediaminetetraaceticacid (EDTA, 351-027-721; Quality Biological) was added to the solution. The plate was then placed on a shaker at 4°C for 30–60 min. The plate was checked every 15–30 min to confirm the absence of crypts from the intestinal tissue under the microscope.

The remainder of the steps in the protocol was performed in a sterile culture hood. Once the crypts had dissociated from the intestine, the tissue and complete chelating solution were transferred back into a 15-mL conical tube. Five milliliter of complete chelating solution was added for a total volume of 8 mL and this was vigorously triturated 20 times. Afterward, 2 mL of FBS was added for a total volume of 10 mL and this was pipetted up and down once. The tissue was allowed to settle on ice for about 1 min. Then, the supernatant containing the crypts was aspirated off and transferred through a 70 μm filter by gravity. The filtered supernatant was centrifuged at 750 $g \times 5$ min. After centrifugation, the supernatant was aspirated, and the pellet resuspended in 10 mL of CMGF– media and pipetted up and down six times. The cells were then placed on ice for 30 min to allow them to settle, after which the supernatant was carefully removed leaving behind 2 mL of CMGF–. Then, more CMGF– media were added to bring the volume back up to 10 mL, and the solutions was centrifuged at 750 $g \times 5$ min.

After centrifugation, all of the supernatant was aspirated, and the crypts were resuspended in Matrigel. The volume of Matrigel varied depending on the number of mice used, although 30 μL is needed per well of a 24-well plate, and typically 6 wells were obtained per mouse. Thus, usually 180 μL of matrigel was used. The cells were plated into 24-well plates and the Matrigel allowed to gel in the cell incubator at 37°C for 5–10 min. After gelling, 0.5 mL of warm CMGF+ media was added to each well.

Enteroids were maintained in either CMGF+ media or mouse minimal media. The media were changed every 2–3 days and the cells were subcultured once per week as described.[24–27] Enteroids were passaged by scraping the cells and Matrigel off the bottom of the well (with mini scrapers, 22003; Fisher Scientific) and placing into a conical tube. The cells and Matrigel were centrifuged at 750 $g \times 5$ min, the supernatant aspirated, and then 1–2 mL of TrypLE added (Thermofisher; 12605028). The cells were incubated in TrypLE for 5 min at 37°C. Afterward, the enteroids were triturated 15–20 times with a P1000 pipette. After trituration, 8–9 mL of CMGF– media was added and the enteroids centrifuged at 750 $g \times 5$ min. After centrifugation, the supernatant was aspirated, the enteroids were suspended in an appropriate volume of Matrigel (depending on the number of wells to be plated), and the enteroids plated into 24-well plates. The plates were next placed in the incubator at 37°C to allow the Matrigel to harden. Afterward, 0.5 mL of CMGF+ or mouse minimal media containing 10 μM Y-27632 compound, which is a rho-associated, coiled-coil-containing protein kinase (ROCK) inhibitor, was added to each well. The enteroids were left in this media for 3 days, after which, every other day media change resumed. With this subculturing technique, enteroids were typically passaged at a ratio of 1:6.

MTT assay

MTT assay was used as a measure of cytotoxicity of PGS scaffolds as described.[33] Caco-2 cells were removed from the flasks with 0.25% (v/v) trypsin and 0.02% EDTA solution in $1 \times$ phosphate-buffered saline (PBS) and adjusted to a concentration of 1×10^6 cells/mL in media. PGS scaffolds with varying concentrations of MDI were seeded with 50 μL cell suspension, followed by a 30-min period without additional media to enable cell attachment. Cells were cultured for 1 week to enable scaffold coverage. Caco-2 cells were enzymatically removed from scaffolds and adjusted to a concentration of 1×10^5 cells/mL in media. One hundred microliter cell suspension was added to 96-well plates and cultured for 48 h, before performing an MTT Assay (Thermofisher; cat V13154) according to manufacturer's instructions.

In vitro *degradation of scaffold*

Degradation of the scaffold was measured as change in mass of the scaffolds over time in both cell culture media and digestive media. Digestive media consisted of bile salts and pancreatic enzymes (2.4 mg/mL porcine bile extract, B8631; Sigma; 0.4 mg/mL pancreatin, P7545; Sigma; 100 mg/mL $NaHCO_3$, and dH_2O, pH 6.5). Scaffolds were incubated at 37°C in cell culture media or digestive media. At weekly intervals, scaffolds were removed from solution and weighed. Scaffold degradation was determined according to mass loss.

In a separate experiment, scaffolds underwent seeding with GFP-enteroids. The structural and mechanical properties of the seeded scaffolds, in addition to scaffolds maintained in cell culture media and digestive media, were determined over time (2, 4, and 6 weeks). At each time point, scaffolds underwent rheometer testing (described below, $n = 3$–4 per group per time point), evaluation with SEM ($n = 4$), and confocal microscopy ($n = 4$). Scaffolds for rheometer testing were punched into 25 mm diameter circles. Scaffolds for imaging were punched into 8 mm diameter circles and at the end of each time point were cut in half and processed for either SEM or confocal microscopy.

The microstructural degradation was determined from the SEM images. Scaffold parameters were measured at baseline, 2, 4, and 6 weeks. Images were taken of the scaffolds from the top and side to measure the following parameters: scaffold base thickness, villus height, the width of the villi at the base, the width of the villi at the top, and the spacing between the villi. Measurements were taken using Fiji.[34] The number of scaffolds analyzed for each parameter at the baseline time point was 11–12 with an average of 49 images analyzed and an average of 165 independent measurements performed. Similarly, for each time point, an average of four scaffolds was analyzed with an average of 17 images and 58 independent measurements per parameter. Note that only intact villi were analyzed.

Tensile testing of scaffolds and porcine intestine

Scaffolds were maintained moist in PBS and at room temperature. Dog-bone die specimens were cut out according to ASTM D638 standard using die type V (width = 3.18 mm and gauge length = 7.62 mm, purchased from Pioneer-Dietecs). The thickness of the scaffolds was measured using an inverted microscope (Leica DMi8A, Wetzloar, Germany).

Each specimen had three images obtained with three measurements obtained per image. These measurements were averaged to obtain the averaged thickness of the scaffold specimens. For villus scaffolds, the thickness was measured from the flat surface to the base of the villi. A total of 10 villus scaffolds and 5 nonvillus scaffolds were tested each in triplicate (30 specimens and 15 specimens, respectively). Any specimen that did not fail in the narrow section of the specimen was excluded from analysis.

For mechanical testing, porcine intestine was collected from 21-day-old male pigs with an average weight of 4.02 kg (0.19 kg) after being euthanized as part of a cardiopulmonary resuscitation model. Intestine was obtained within 2 h of death. When isolating the intestine, the mesentery was carefully removed, and the intestine was opened longitudinally along the mesenteric border and cleansed by washing with Hank's Buffered Salt Solution (HBSS). Specimens were maintained in HBSS on ice until ready for preparation. Before testing, specimens were warmed to room temperature. The thickness of the intestine was measured in three places along its length using calipers and these thicknesses were averaged. The averaged thickness was assumed to be the idealized thickness of the entire length of tested intestine. Next, dog-bone specimens were cut from the intestine using the aforementioned die in a longitudinal manner. These specimens were then mounted on a cardboard mount to assist in loading them into the MTS device. A total of six different animals were tested each in triplicate. All testing was completed within 8–10 h of death.

Tensile testing was performed with an MTS Criterion Model 43 Device using a 100 N load cell as described.[35] All tests were performed with a crosshead speed of 10 mm/min and carried out until the specimens failed. The gage length was defined as that of the specimen die, that is, 7.62 mm. Maximum load and ultimate tensile strength (UTS) were calculated by the MTS software. Young's modulus was calculated by the MTS software using toe compensation for the intestinal tissue. Strain at failure was defined as a 40% decrease in load from the maximum load for all specimens. Stress–strain curves for all specimens were subsampled for every 0.005 mm/mm of strain using MATLAB and subsequently averaged.

Rheometer measurements

Viscoelastic properties of the scaffolds were measured with an Anton Paar Modular Compact Rheometer Model 302. Scaffolds were measured at baseline after fabrication ($n=4$ tested in triplicate), and after 2, 4, and 6 weeks of culture in various conditions: culture media only ($n=4$), digestive media only ($n=4$), and seeded with GFP-enteroids ($n=3$). Digestive media consisted of bile salts and pancreatic enzymes (2.4 mg/mL porcine bile extract, B8631; Sigma; 0.4 mg/mL pancreatin, P7545; Sigma; 100 mg/mL $NaHCO_3$, dH_2O, pH 6.5). For rheometer testing, a 25-mm diameter punch was used to cut scaffolds. For specimens undergoing SEM and confocal microscopy analysis, 8-mm diameter punches were used. Scaffolds were seeded as described below with the following modifications: the 25-mm scaffolds were coated in 3 mL of type I collagen and seeded with 730,000–4,900,000 GFP-enteroids (passage 7–9) per scaffold in 0.5–1 mL of mouse minimal media plus ROCK inhibitor. The 8-mm scaffolds were coated with 0.5 mL of type I collagen and seeded with 75,000–490,000 enteroids per scaffold in 50 μL of mouse minimal media plus ROCK inhibitor. The scaffolds were then incubated for 1 h at 37°C in the incubator before adding the final volume of media (3 mL for large scaffolds and 0.5 mL for small scaffolds). Twenty-five millimeter specimens were maintained in six-well plates in 3 mL of the respective media (media or digestive media) per well and 8-mm scaffolds were maintained in 24-well plates with 0.5 mL of media per well. All media were changed every other day. Testing parameters were determined with preliminary tests on scaffolds and frequency sweeps were performed with 0.1% strain (determined to be in the linear elastic region on amplitude sweeps) from 10 to 0.1 Hz. Subsequently, scaffolds underwent stress relaxation testing with a strain of 1%, which was maintained for $\sim$1000 s.

Scaffold seeding

Scaffolds were first cut to the desired size (either 8-mm diameter or 25-mm diameter circles). The scaffolds were then sterilized in 70% ethanol for 2 h at room temperature. Next, they were rinsed in PBS 5×20 min at room temperature. Then the scaffolds were coated in 200 μg/mL of type I collagen (rat tail, 354236; BD Biosciences) for 2 h in an incubator at 37°C (0.5 mL for 8-mm scaffolds and 3 mL for 25-mm scaffolds). Note, the type I collagen was made into a 1 mg/mL stock by diluting in 100 mM acetic acid. Then, the final 200 μg/mL concentration was prepared by diluting the stock solution in sterile water. The scaffolds were then rinsed with CMGF− media at least thrice to ensure the dilute acetic acid from the collagen had been washed away (determined by the absence of phenol red indicator color change). Mouse minimal media were then applied to the scaffolds (0.5 mL for 8-mm scaffolds and 3 mL for 25-mm scaffolds) for 1 h at 37°C in the incubator. Next, the enteroids were passaged and resuspended in mouse minimal media plus ROCK inhibitor (50 μL of media per scaffold to be seeded). The enteroids were statically seeded on top of the scaffolds and placed in the incubator at 37°C for 1 h to allow the cells to attach. After 1 hour, the remainder of the media was added to bring the volume to 0.5 mL per well. The seeded scaffolds were maintained in this medium for 3 days before the first medium change, and then afterward, the medium was changed every other day. All GFP and C57 enteroids used for seeding were between passages 8 and 19.

Mouse omental implantation

Mice 57–92 days old were used for implantation of the scaffolds into the omentum as described.[17] Mice received either GFP-enteroid seeded scaffolds or scaffolds alone. All scaffolds had undergone sterilization as described in the scaffold seeding section and were then either seeded with cells or maintained without cells in the same culture medium until the time for implantation. After implantation, mice were euthanized at 2-, 4-, 8-, and 12-week time points. Six mice were used per group per time point (3 males and 3 females per group) for a total of 48 mice.

For surgery, the mice were anesthetized with isoflurane (1–3% for induction and maintenance). While under anesthesia, all mice were weighed, clipped of fur, and eyes lubricated with a petrolatum ophthalmic ointment (Puralube®

Vet Ointment, 17033-211-38). The abdomen was sanitized using povidone-iodine. Then, the abdomen was opened sharply and the omentum identified. A 4-0 prolene was placed in the scaffold as a marking stitch, and then it was placed in the abdomen under the omentum as described.[17] The abdomen was then closed in layers, the muscle layer and skin, using 4-0 absorbable sutures. Postoperatively, the mice received 0.1 mg/kg buprenorphine subcutaneously for pain management and were monitored until awake and ambulatory.

In vivo *degradation*

After scaffolds were removed from the mice, they were processed for SEM as described above. The SEM images were then analyzed in a similar manner as described in the *in vitro* degradation section, except only scaffold thickness and villus height were measured due to some difficulty in degradation of the scaffolds, preventing more detailed measurements and the presence of tissue obscuring the view for detailed measurements. For each parameter (i.e., thickness and villus height), at least two scaffolds (range 2–6) were evaluated with an average of 14 images, and an average of 42 and 24 independent measurements was made for thickness and villus height, respectively.

Histology, immunohistochemistry, and microscopy

Seeded scaffolds were fixed in 4% paraformaldehyde (15710; Electron Microscopy Sciences, Hatfield, PA) diluted in PBS for 1 h to overnight at room temperature, similar to previously described methods.[36] They were subsequently washed with PBS and then immunostained following standard protocols. In cases where fixation occurred overnight, scaffolds underwent antigen retrieval using citric acid (pH 6). Primary antibodies were used at 1:250 dilution and incubated overnight. After rinsing with PBS plus Tween, the scaffolds were counterstained with 4′, 6-diamidino-2-phenylindole dihydrochloride (DAPI, 422801; Biolegend) and secondary antibodies at a dilution of 1:1000 overnight. In some cases, phalloidin (ThermoFisher Scientific; R415) was used and was added with the secondary antibodies at a dilution of 1:1000. The scaffolds were then rinsed and imaged in bloc. The following primary antibodies were used: Ki67 (Abcam; ab15580), E-cadherin (R&D Systems; AF748), sucrase-isomaltase (Santa Cruz; sc27603), and chromogranin A (Abcam; ab15160). The secondary antibodies used were as follows: Alexa Fluor 488 AffiniPure F(ab′)2 fragment donkey anti-rabbit immunoglobulin G (IgG, 711-546-152; Jackson Immunoresearch) and Cy5 AffiniPure donkey anti-goat IgG (Jackson Immunoresearch; 705-175-003).

Explanted constructs were fixed in 4% paraformaldehyde at 4°C at least overnight. They were then equilibrated in 30% sucrose solution to prevent freeze artifact. Next, they were embedded in gelatin to prevent the scaffolds from lifting off the slides when staining. This was done by incubating the samples for 2 h at 45°C in a 5% (w/w) porcine gelatin (Sigma, St. Louis, MO; G1890, Lot SLBC8470V) solution with 5% (w/w) sucrose (57-50-1; Affymetrix, Cleveland, OH) (i.e., 2.5 g of gelatin and 2.5 g sucrose in 45 mL of water) in cryosectioning molds covered with parafilm. After incubation, the parafilm was removed and the samples were placed in a −20°C freezer overnight to harden. The following day, the samples were removed from the molds, the gelatin trimmed, and then the gelatin/construct specimen embedded in optimum cutting temperature freezing medium for frozen histology and frozen in liquid nitrogen. The samples were then stored at −80°C until cryosectioning. The constructs were sectioned using standard techniques at a thickness of 10 μm.

Histologic sections were stained for hematoxylin and eosin (H&E) and Alcian blue staining. They also underwent immunohistochemical (IHC) staining. For IHC staining, samples were rinsed with PBS containing (0.05% tween-20), underwent antigen retrieval with citric acid (pH 6.0), primary antibody incubation overnight at 4°C, and then secondary antibody incubation for 2 h at room temperature. DAPI counterstain was included with the secondary antibody incubation diluted 1:1000. All primary antibodies were diluted 1:250, except for P75, which was diluted 1:500. The primary antibodies used were as follows: GFP (Millipore; AB3080 and Santa Cruz; sc73556), sucrase-isomaltase (Santa Cruz; sc27603), lysozyme (Santa Cruz; sc27958), chromogranin A (Abcam; ab15160), E-cadherin (R&D Systems; AF748), Lgr5 (MBL Life Science; LS-A1236), CD31 (BD Pharmingen; 550274), Ki67 (Abcam; ab15580), vimentin (Santa Cruz; sc7558), α-smooth muscle actin (Sigma-Aldrich; A5228), F4/80 (Abcam; ab16911), CD206 (Abcam; ab64693), CD45 (Abcam; ab25386), CD86 (Biolegend; 105002), myeloperoxidase (Santa Cruz; sc34161), Sox10 (R&D Systems; AF2864), glial fibrillary acidic protein (Agilent; Z033429), and P75 (Abcam; ab8875). All secondary antibodies were diluted 1:1000 and those used were as follows: Alexa Fluor 555 donkey anti-mouse IgG (Life Technologies; A31570), Alexa Fluor 594 donkey anti-rat IgG (Life Technologies; A21209), Alexa Fluor 488 AffiniPure F(ab′)2 fragment donkey anti-rabbit IgG (Jackson Immunoresearch; 711-546-152), and Cy5 AffiniPure donkey anti-goat IgG (Jackson Immunoresearch; 705-175-003).

Confocal microscopy images were obtained using a Nikon Eclipse Ti microscope (Nikon, Melville, NY). Fluorescent microscopy images were obtained using a Leica DMi8 microscope. Images were analyzed and processed using Fiji[34] with the Image5D plugin.

Statistical analysis

Where appropriate, and as indicated with each figure, statistical analysis was performed. All statistical analyses were formed with GraphPad Prism 7.0c (GraphPad Software Incorporated, La Jolla, CA). Normal distributions were assumed and either an analysis of variance (ANOVA, one-way or two-way as appropriate) with Bonferroni-corrected *post-hoc* *t*-tests or two-tailed *t*-tests was used as appropriate. Statistical significance was taken as a p-value <0.05.

Results

PGS scaffolds mimic native intestinal microarchitecture

We first showed that scaffolds could be successfully fabricated using PGS and that they displayed a microarchitecture that mimicked the dimensions of native intestine. Concentrations of 2%, 4%, and 6% MDI were used for the villus portion and these concentrations were tested for porosity and found to have similar values (74% ± 2.6%, 69% ± 3.9%, and 67% ± 1.5%, respectively, Fig. 1A). The 2%

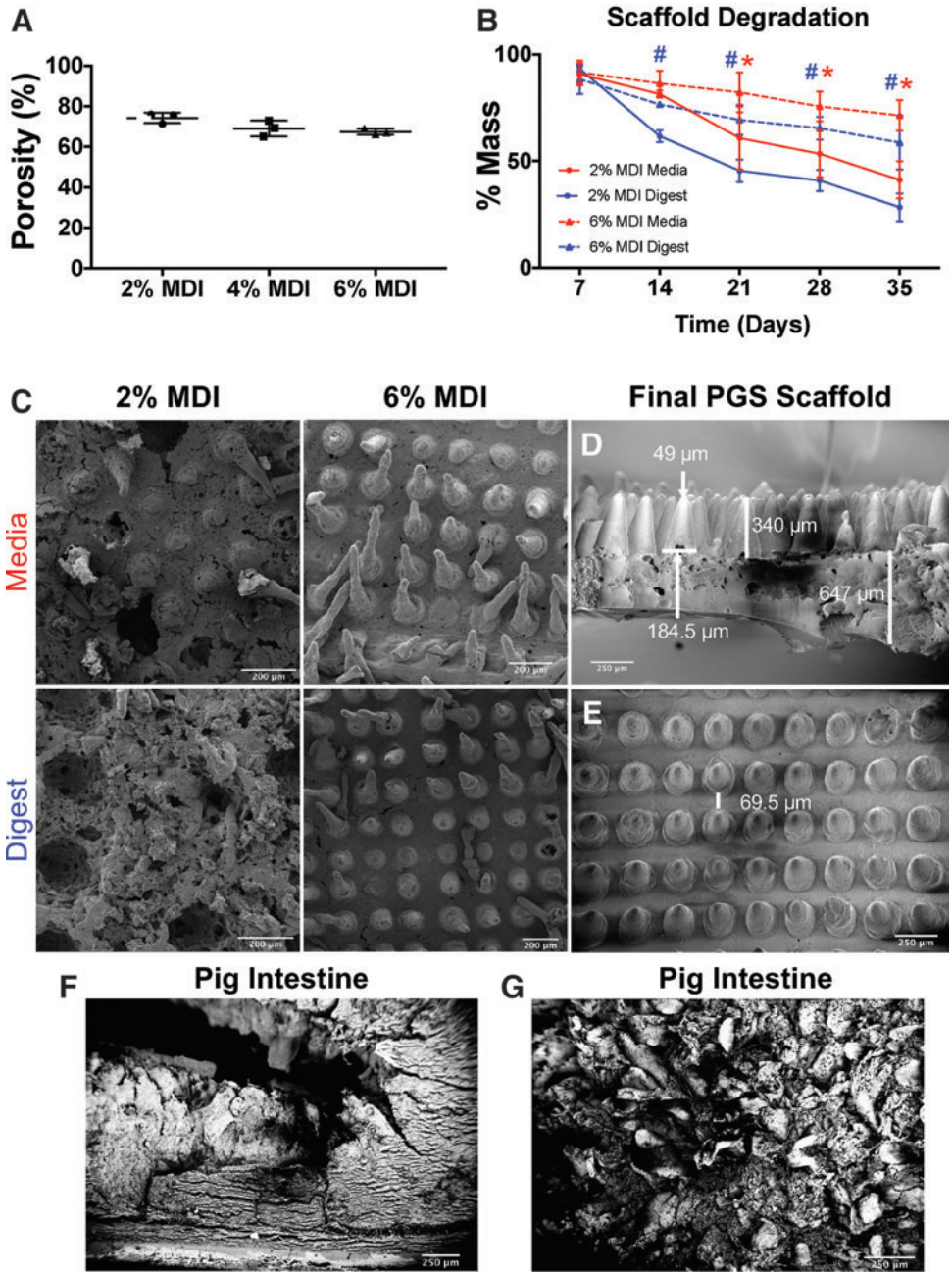

FIG. 1. Characterization of scaffold porosity and degradation with various concentrations of MDI crosslinker used in the villus layer of the scaffold. **(A)** Scaffold porosity was not significantly different between the different MDI concentrations. **(B)** Mass loss of scaffolds after 35 days (5 weeks) of *in vitro* degradation. Six percent MDI had slower degradation compared to 2% in both media and digestive media. The differences were statistically different in media between 2% and 6% MDI at 21, 28, and 35 days with *p*-values of 0.0252, 0.202, and 0.0013, respectively (indicated by *red* *). Statistical differences existed in the digestive media at 14, 21, 28, and 35 days with *p*-values of 0.0439, 0.0007, 0.0005, and <0.0001, respectively (indicated by *blue* #). **(C)** SEM images of 2% MDI and 6% MDI after 35 days of degradation in media versus digestive media demonstrating that the 2% MDI scaffolds lost their structural integrity in both conditions, while the 6% MDI maintained architectural integrity in both conditions. **(D)** Side-view SEM of the final poly(glycerol sebacate) scaffold used in the remainder of the studies with the shown dimensions. This scaffold was bilayered with 6% MDI crosslinker used in the villus portion and 2% MDI crosslinker used in the base section. **(E)** Top-view SEM of the final scaffold chosen. **(F)** SEM cross-section of native porcine intestine for comparison. **(G)** En face SEM view of native porcine view demonstrating villi for comparison. MDI, 4,4′-methylenebis(phenyl isocyanate); SEM, scanning electron microscopy. Color images are available online.

MDI and 6% MDI concentrations were then tested for *in vitro* degradation by evaluating the degree of mass loss, and SEM for visualization of the degradation changes because they were the initial two extremes of crosslinking (Fig. 1B, C). As shown in Figure 1A and B, we determined that 2% MDI scaffolds had only 41% (±8.8%) and 28.3% (±6.6%) mass remaining in media and digestive media compared to 71.4% (±7.2%) and 58.7% (±12.7%) mass remaining in the 6% MDI scaffolds in media and digestive media, respectively (Fig. 1B). There was a statistical difference in mass loss between 2% and 6% MDI in the medium conditions starting at 21 days and continuing at 28 and 35 days (p values 0.0252, 0.202, and 0.0013, respectively). For the digest conditions, there was a statistically significant difference between 2% and 6% MDI at 14, 21, 28, and 35 days (p values 0.0439, 0.0007, 0.0005, and <0.0001, respectively). These findings were confirmed with SEM (Fig. 1C), which demonstrated maintenance of the villus structures in the 6% MDI scaffolds after 5 weeks of *in vitro* degradation in both cell media and digestive media compared to complete loss of villus structures in the 2% MDI scaffolds.

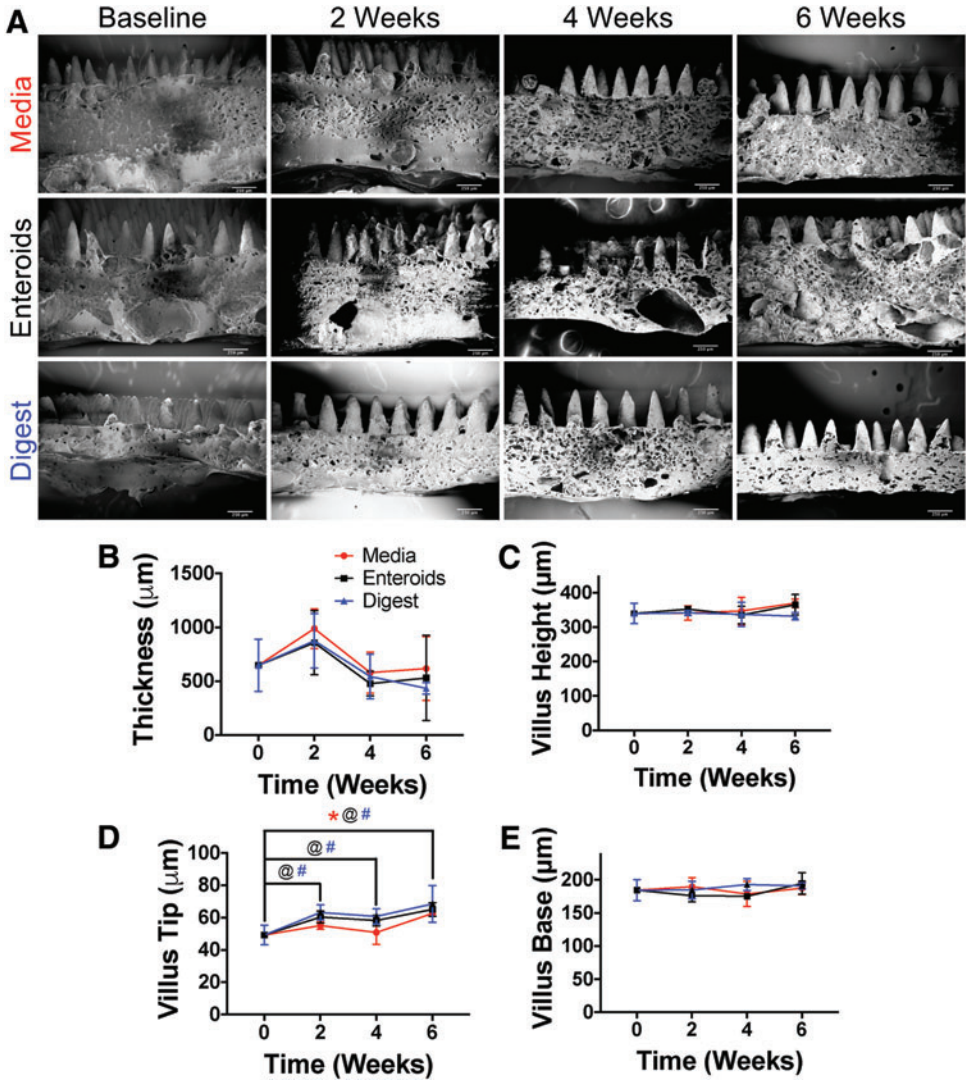

FIG. 2. Image analysis of microarchitectural changes to scaffolds with 6% MDI crosslinking in the villus layer and 2% MDI in the base layer during *in vitro* degradation. **(A)** SEM of the scaffolds at each time point in media alone, seeded with enteroids, and in digestive media (scale bars = 250 μm). The overall dimensions and villus architecture are maintained. **(B–E)** The quantification of the image analysis. For thickness, there was a statistically significant variation in time ($p = 0.0012$), but on *post-hoc* comparison of each time to baseline within each group, there were no statistical differences. There were no differences for villus height. There were significant differences in villus tip in both the time and group variables ($p < 0.0001$ and $p = 0.0113$, respectively). On multiple comparisons, there was a difference in the media group between 0 and 6 weeks ($p = 0.0007$), in the enteroid group between baseline and 2, 4, and 6 weeks ($p = 0.0056$, 0.0318, and <0.0001, respectively), and in the digest group, there were differences for each time point (2, 4, and 6 weeks) compared to baseline ($p = 0.0004$, 0.004, and <0.0001, respectively). Regardless of the statistical differences, these changes in size were small and in many cases, there were increases in dimension, which more likely represents either measurement error or some other artifact. @, #, and * indicate statistical significance. @ represents differences between time points for enteroids, # represents differences between time points for digest group, and * indicates difference in time points for media group. Color images are available online.

Based on these results, we chose scaffolds with 2% MDI crosslinker in the base and 6% MDI crosslinker in the villus portion for all subsequent studies. When characterizing these scaffolds with SEM, they had the following dimensions (±standard deviation, Fig. 1D, E): thickness of 647 μm (±241 μm), villus height of 340 μm (±29.5 μm), width of the base of the villus of 184.5 μm (±16 μm), width of the villus tip of 49 μm (±6 μm), and spacing of 69.5 μm (±11 μm). As a comparison, SEM of native porcine intestine is demonstrated in Figure 1F and G. Taken together, these experiments revealed that PGS scaffolds with 2% MDI crosslinker in the base and 6% MDI crosslinker in the villi were most suitable for the remainder of our studies. We therefore next evaluated the ability of this scaffold composition to maintain its structure when exposed to various *in vitro* conditions.

PGS scaffolds maintain their structure during in vitro *exposure to cell media and media with digestive enzymes, or when seeded with intestinal stem cells*

We next sought to characterize how the microarchitecture of the scaffolds would change over time during *in vitro* degradation under three conditions: cell culture media alone, seeded with enteroids, or in digestive media (Fig. 2). Over 6 weeks, in all conditions, there were no observable change in scaffold thickness, villus height, width of the villus base, or width of the villus tip as evidenced on SEM (Fig. 2A). On image analysis, there were statistically significant differences in scaffold microarchitecture, which were due to expected measurement variation (Fig. 2B–E). In particular, the thickness of the scaffolds showed a significance in variation over time ($p=0.0012$) in two-way ANOVA, but on multiple comparisons with each time point compared to baseline, there were no statistically significant differences. Villus height had no statistically significant variation in two-way ANOVA. Villus tip dimensions showed statistically significant variation in both time ($p<0.0001$) and treatment group ($p=0.0113$) in two-way ANOVA. In multiple comparisons, in which each time point was compared to baseline within groups, the following statistical differences were found (Fig. 2D): in the media group 6 weeks was statistically different from baseline ($p=0.0007$), in the enteroid group 2 versus 0 weeks ($p=0.0056$), 4 versus 0 weeks ($p=0.0318$), and 6 versus 0 weeks ($p<0.0001$), and finally in the digest media group 2 versus 0 weeks ($p=0.0004$), 4 versus 0 weeks ($p=0.0040$), and 6 versus 0 weeks ($p<0.0001$). For villus base, there were no statistically different variations in two-way ANOVA. Based upon these findings, we next sought to determine the tensile properties of the scaffolds compared to native intestinal tissue.

PGS scaffolds approach the mechanical properties of native porcine intestine

We next evaluated the tensile properties of the scaffolds compared to native porcine intestine with the goal to evaluate the degree to which the synthetic intestinal scaffolds could approximate native intestinal properties (Fig. 3). Because of concern that the villus structures in the scaffold might serve as weak points in the scaffold, which could cause early failure, we also tested scaffolds without villi (which were crosslinked with 2% MDI in the base, the same concentration that is used for the base in villus scaffolds) in comparison with those containing villi. Importantly, there were no significant differences detected when comparing the stress–strain curves of villus scaffolds to flat scaffolds (Fig. 3A) as well as maximum load (3.19 ± 1.31 N vs. 2.89 ± 1.35 N), UTS (1.44 ± 0.60 MPa vs. 1.56 ± 0.42 MPa), Young's modulus (5.60 ± 5.05 MPa vs. 3.62 ± 1.36 MPa, E), and strain at failure (77.21 ± 19.84% vs. 102.7 ± 15.8%) (Fig. 3B–E).

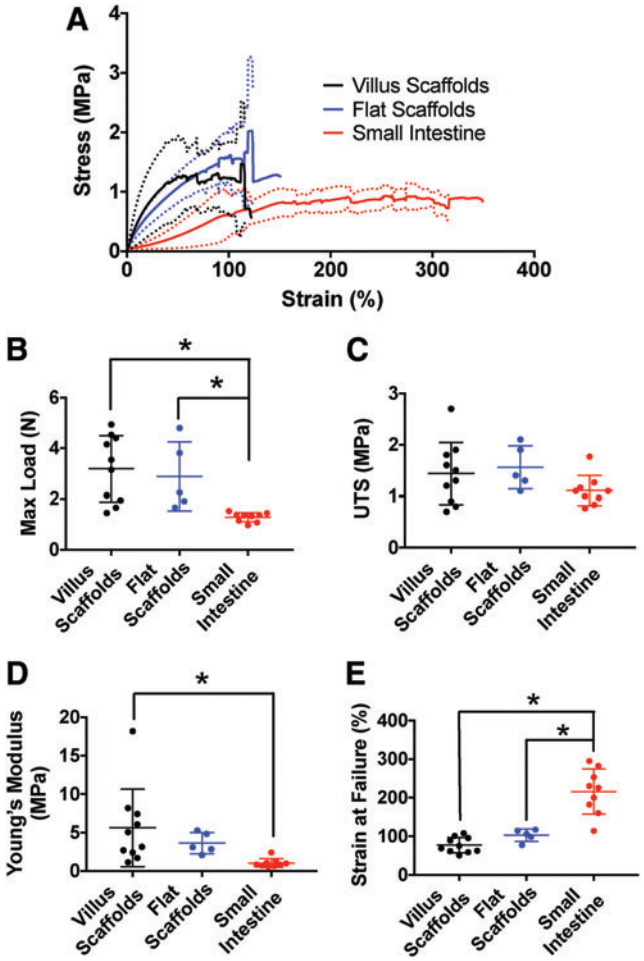

FIG. 3. Tensile properties of the scaffolds compared to native porcine intestine. **(A)** Average stress–strain curves of scaffolds with villi ($n=10$), scaffolds without villi ($n=5$), and native porcine small intestine ($n=9$). The *solid lines* represent the average stress–strain curve and the *dotted lines* represent plus or minus one standard deviation. The tensile properties between the villus scaffolds and flat scaffolds are nearly identical, indicating that the addition of the villi does not result in stress concentrations and earlier failure. Villus scaffolds have tensile properties that are on the same scale as native intestine, but they do not match native intestine. **(B)** Maximum load for each group. Both the villus and flat scaffolds had statistically significantly higher maximum load compared to native intestine ($p=0.0022$ and 0.0373, respectively). **(C)** UTS was not statistically different between groups. **(D)** Young's modulus **(E)** was statistically significantly higher in the villus scaffolds compared to the small intestine ($p=0.0231$). **(E)** Strain at failure was statistically significantly lower in villus and flat scaffolds compared to native small intestine ($p<0.0001$ and 0.0001, respectively). UTS, ultimate tensile strength. *indicates statistical significance. Color images are available online.

When comparing the stress–strain curve of the villus scaffolds to native porcine intestine, the tensile behavior is clearly different. In particular, the scaffolds are stiffer with a higher E (5.60 ± 5.05 MPa vs. 1.03 ± 0.57 MPa, $p = 0.0231$) and maximum load (3.19 ± 1.3 N vs. 1.29 ± 0.18 N, $p = 0.0022$), but lower strain at failure ($77.21 \pm 19.84\%$ vs. $215.9 \pm 58.47\%$, $p < 0.0001$) compared to native intestine (Fig. 3A). These differences were statistically significant (Fig. 3B–E). The scaffolds also had a higher UTS (1.44 ± 0.60 MPa vs. 1.11 ± 0.29 MPa), but the difference was not statistically significant. Of note, there were also statistically significant differences between the flat scaffolds and native intestine for maximum load (2.89 ± 1.36 N vs. 1.29 ± 0.18 N, $p = 0.0373$) and strain at failure ($102.7 \pm 19.84\%$ vs. $215.9 \pm 58.47\%$, $p = 0.0001$). Thus, the tensile properties where shown to be on the same order of magnitude as that of native porcine intestine. In addition, from a practical point of view, qualitatively, the scaffolds were easy to handle, could be easily rolled into tubes, and held sutures well. Therefore, the scaffolds were felt to mimic the biomechanical properties of native intestine enough to be evaluated further for the generation of an artificial intestine.

PGS scaffolds maintain their mechanical properties during in vitro *exposure to cell media and media with digestive enzymes, or when seeded with intestinal epithelial stem cells*

In addition to ensuring that the scaffolds had similar tensile properties to native intestine, we next sought to characterize how those properties changed over time with exposure to *in vitro* conditions that could induce matrix degradation. This was tested with rheometer analysis using three *in vitro* conditions: scaffolds maintained in cell culture media, scaffolds seeded with enteroids, and scaffolds maintained in digestive media. There did not appear to be any differences in storage modulus between any of the groups and baseline testing (Fig. 4A–C and G), indicating that the scaffolds maintained their elasticity during exposure to cell media and digestive media, which mimic the intestinal succus, and when seeded with intestinal epithelial stem cells.

In contrast, the loss modulus consistently increased with time (Fig. 4D–F and H), suggesting an increasing viscous component to the viscoelastic properties under the three conditions. This finding may have been due to a loss of crosslinking over

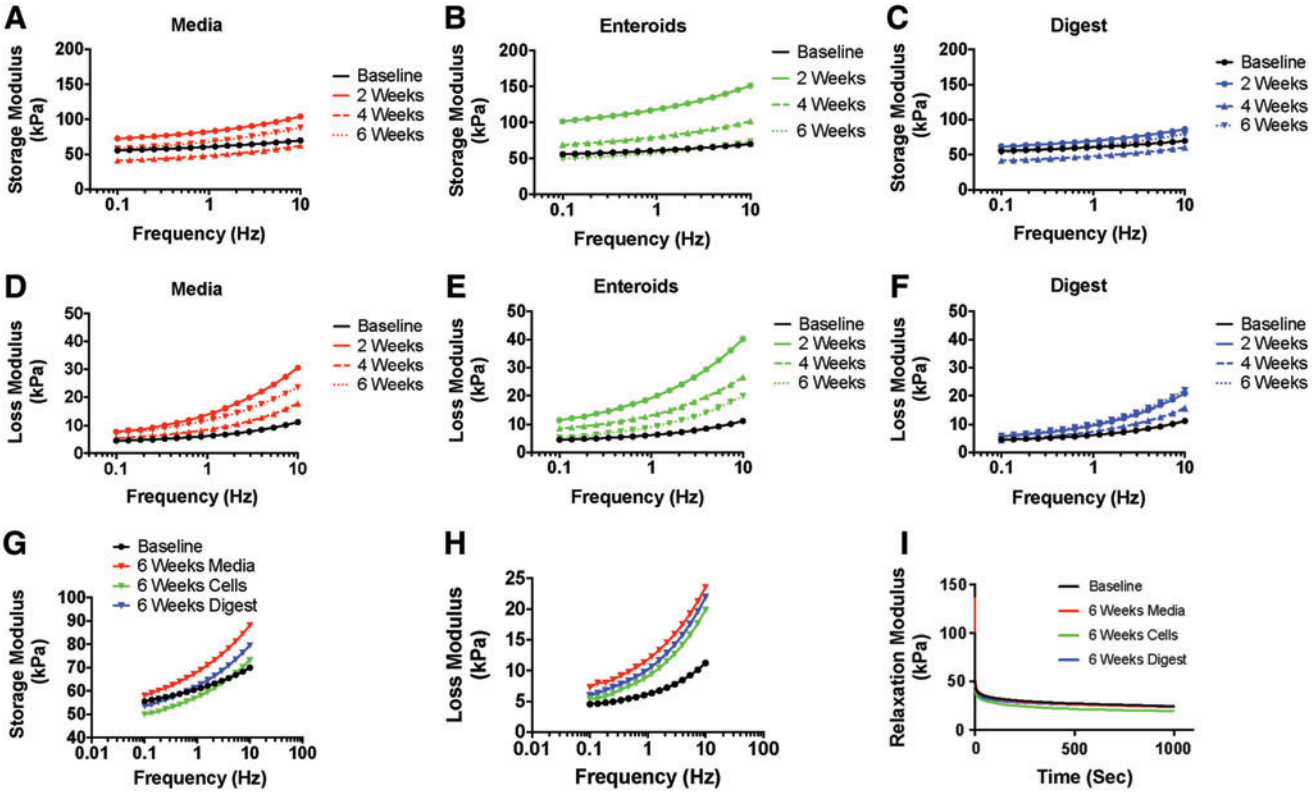

FIG. 4. Rheologic properties of the scaffolds over time during *in vitro* degradation. **(A–C)** Average storage moduli of the scaffolds at each time point in each condition. In general, the storage moduli were the same over time and across groups, indicating that the scaffolds maintained their elasticity. **(D–F)** Average loss moduli of the scaffolds at each time point in each condition. Again, the scaffolds had similar loss moduli across groups at baseline. Over time, however, there seemed to be an increase in loss modulus, indicating an increase in the viscous component of the scaffold likely due to a decrease in crosslinking over time. **(G)** Demonstrates the average storage moduli of the scaffolds in each group after 6 weeks compared to baseline. There were no noticeable changes. **(H)** Demonstrates the average loss moduli of the scaffolds in each group after 6 weeks compared to baseline, which showed an increase in loss modulus in all groups. **(I)** Average stress-relaxation curves of the scaffolds in each group at 6 weeks compared to baseline, demonstrating that there were no changes in stress-relaxation behavior. Note that statistical comparison was not performed on the rheologic parameters. Color images are available online.

time as the scaffolds start to degrade. Of interest, there did not seem to be noticeable differences in rheometer properties between groups (i.e., the scaffolds behaved similarly regardless of whether they were maintained in media, seeded with cells, or maintained in digestive media), thus indicating that the scaffolds may be able to readily withstand the more hostile *in vivo* environment. Finally, there were no differences observed in the stress-relaxation behavior of the scaffolds at any time point or under any condition tested (Fig. 4I).

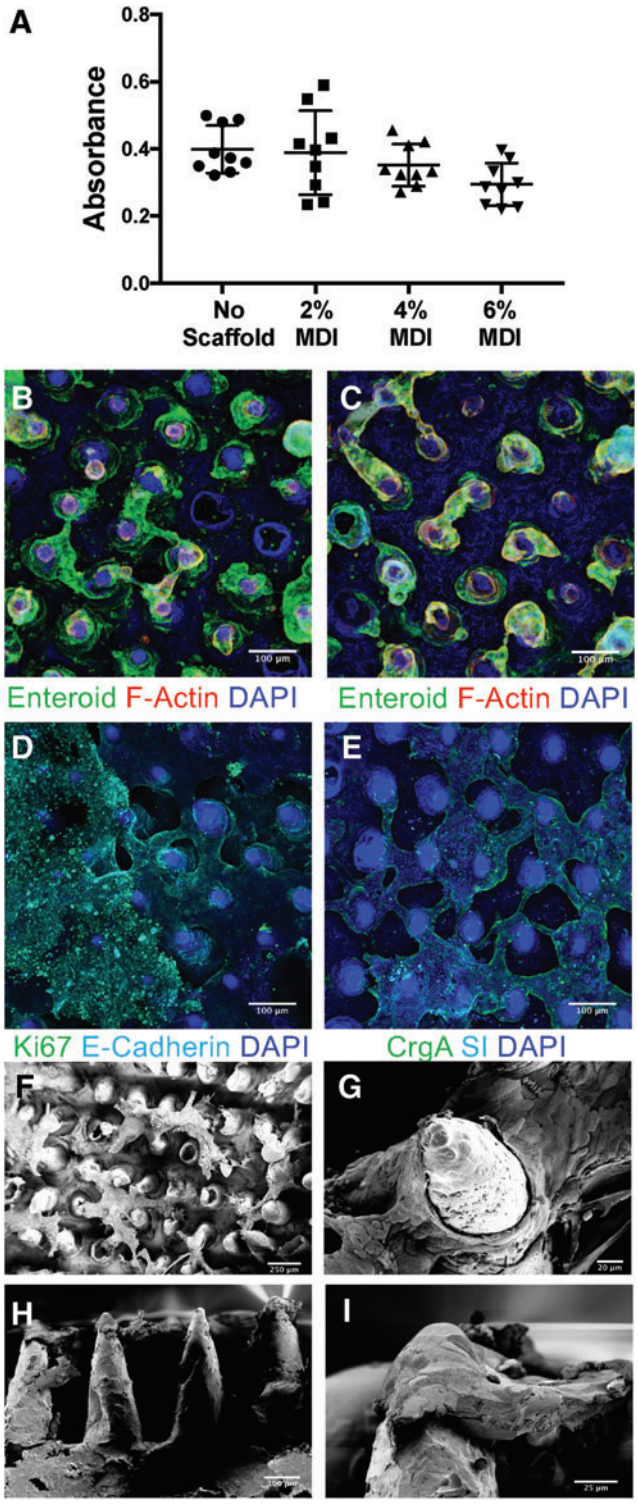

PGS scaffolds are cytocompatible and accommodate intestinal epithelial stem cells

To assess whether the villus scaffolds could serve as appropriate scaffolds for artificial intestine, we next sought to confirm that the scaffolds were cytocompatible and that enteroids could attach to and cover the scaffolds (Fig. 5). Initially, an MTT assay was performed using Caco-2 cells, which demonstrated no differences in compatibility by one-way ANOVA (Fig. 5A). Next, enteroids constitutively expressing GFP (herein called ''GFP-enteroids'') were seeded with PGS villus scaffolds; their detection was improved given their endogenous fluorescence. After growth in culture for 7 days with CMGF+, enteroids were observed to readily attach onto the scaffolds and to cover the villi (Fig. 5B, C), with some cell interactions spanning the intervillus space. To gain insights into the degree to which cells could divide and differentiate on the scaffolds, they were also seeded with wild-type C57Bl/6 enteroids and stained for proliferation (Ki67) and the presence of terminally differentiated cells (chromogranin A for enteroendocrine cells and sucrase-isomaltase for enterocytes) (Fig. 5D, E), which revealed the presence of proliferating cells and a few enteroendocrine cells and enterocytes. The relatively few numbers of terminal intestinal epithelial cells were likely due to the maintenance of the cultures in CMGF+, media that promote stem cell replication and suppress terminal differentiation, with the goal to achieve better coverage of the scaffold.[25,37] We and others have shown that removal of stem cell growth factors results in differentiation of the enteroids (unpublished data; Ladd, M.R., Werts, A.D., Johnson, B., et al.).[25,37] We also evaluated the seeded scaffolds by SEM (Fig. 5F–I), which showed that cells could attach to the villi, and occasionally span across the intervillus space, wrapping around villi, and often capping villi. There were fewer cells penetrating toward the base of the scaffold than expected at the 7-day time point. Based upon these findings, we next sought to evaluate the *in vivo* biocompatibility of the scaffolds, the ability of the scaffolds

FIG. 5. **(A)** MTT assay of Caco-2 cells on scaffolds compared to cells grown without a scaffold. There were no statistically significant differences. **(B, C)** Scaffolds seeded with constitutively expressing green fluorescent protein-enteroids (scale bars = 100 μm). The scaffolds were able to accommodate the enteroids and the enteroids began to attach and cover the villi of the scaffold. **(D, E)** C57 enteroids seeded on the scaffolds (scale bars = 100 μm). **(D)** Enteroids were stained for Ki67 and E-cadherin, demonstrating that the cells continued to proliferate and were of epithelial origin. **(E)** Enteroids were stained for CrgA and SI. There were occasional positively staining cells for both markers, but very few overall, likely due to the fact that the enteroids were maintained in stem cell growth media. **(F)** A top-down SEM of seeded scaffolds demonstrating enteroids attaching to the villi (scale bar = 250 μm). **(G)** A higher magnification SEM of enteroids (scale bar = 20 μm) attaching to and wrapping around a single villus. **(H)** Side-view SEM of seeded scaffold showing enteroids attaching to the tops of the villi in this case (scale bars = 100 μm). **(I)** Higher magnification SEM of the region highlighted in *white* in **(H)** showing the enteroids (scale bar = 25 μm) on top of the villus. CrgA, chromogranin A; SI, sucrase-isomaltase. Color images are available online.

to maintain their properties *in vivo*, and the ability of the seeded scaffolds to form intestinal tissue when implanted.

PGS scaffolds maintain architecture during in vivo *implantation*

Having shown that the scaffolds maintain their properties under various *in vitro* conditions and were able to accommodate seeded intestinal epithelial stem cells, we next sought to evaluate the degree to which the scaffolds maintained their biomechanical properties upon implantation into an animal model. To do this, we implanted scaffolds, either seeded with GFP-enteroids or unseeded, into the omentum of mice for 2-, 4-, 8-, and 12-week time points ($n=6$ per group [seeded vs. unseeded] per time point). At each time point, scaffolds were evaluated grossly and with SEM to assess microarchitecture changes similar to the methods used for *in vitro* degradation (Fig. 6).

On gross examination, the scaffolds maintained their size and shape (Fig. 6A) 12 weeks after implantation. On image

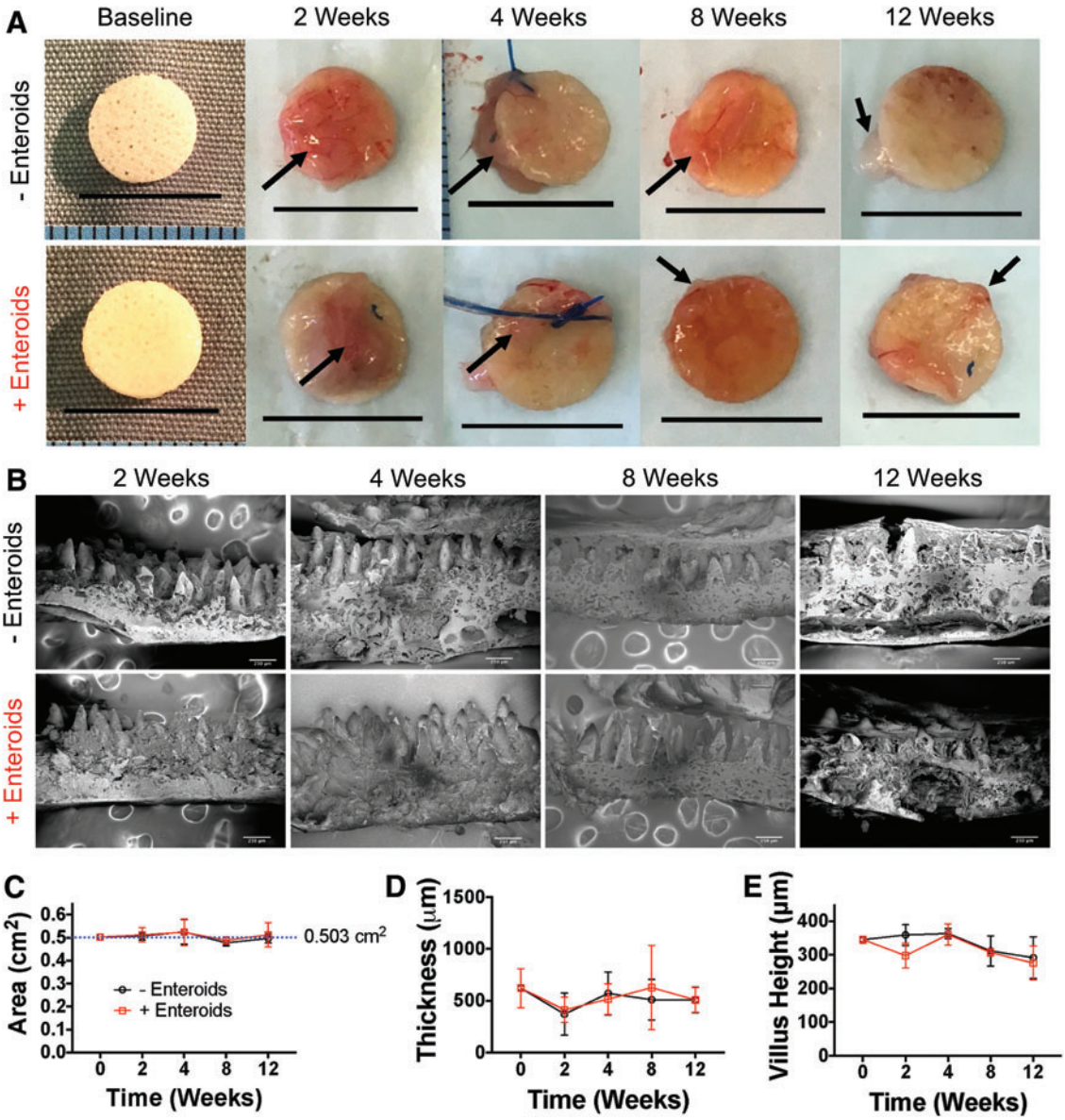

FIG. 6. **(A)** Gross morphology of explanted scaffolds at each time point. Scale bars are 1 cm. There were no observable differences in size or surface area. *Arrows* denote omental tissue that is attached to the surface of the scaffold. **(B)** SEM of scaffolds explanted from each group at each time point (scale bars = 250 μm). There appears to be more tissue attached to the villi at later time points and more broken villi at later time points, but otherwise the microarchitecture appeared preserved. **(C)** Surface area measurements of the scaffolds confirmed that there were no changes in surface area over time, regardless of whether seeded or not. **(D)** Thickness measurements did not demonstrate any change over time. **(E)** Villus height did have a statistically significant difference in variation by one-way analysis of variance in the time variable ($p=0.0027$), but on *post-hoc* multiple comparisons of each time point to baseline within groups, there were no statistically significant differences. Thus, after 12 weeks of omental implantation, there was little evidence of significant degradation by surface area changes or microstructure. Color images are available online.

analysis, there was no statistically significant change in size of the scaffolds from baseline, indicating that they remained intact in the environment of the abdomen (Fig. 6C). On SEM analysis, the microarchitecture was well maintained (Fig. 6B). On image analysis of scaffold thickness, there were no statistically significant changes even at 12 weeks (Fig. 6D). For villus height, there was a statistically different variation in the time variable in two-way ANOVA ($p = 0.0027$), but there were no statistically significant differences in *post-hoc* comparison of each time point to baseline within each group (i.e., −enteroids and +enteroids, Fig. 6E). In many cases, there was a significant amount of tissue noted on top of the scaffolds and some areas where tissue nearly reached the base of the villi. It should be noted that there were many examples of fractured or broken villi to the point that, in some cases, this reduced sample size of samples that could be analyzed, but when analyzing the villi that were intact, there were no changes indicating that the scaffolds have the ability to maintain their architecture for long periods of time *in vivo*.

PGS scaffolds are well tolerated immunologically upon omental implantation

We next assessed the inflammatory response to the implanted scaffolds and the degree to which tissue formation occurred by gross analysis of explanted scaffolds and histologic examination. On gross examination, the scaffolds appeared to be primarily covered by the omentum with some cases involving adhesion to the undersurface of the liver or stomach (Fig. 6A). While inflammation was present, it did not seem severe on gross examination and there did not appear to be any infected implants or abscesses. There did not appear to be differences between seeded or unseeded scaffolds.

Histological analysis confirmed our gross examination findings that there was an inflammatory response and foreign body reaction to the scaffolds (Fig. 7A–E). As could be seen on H&E staining, there was an influx of inflammatory cells at all time points characterized by neutrophils, foreign body giant cells, and fibrosis depending on the time point. This inflammatory response was observed regardless of

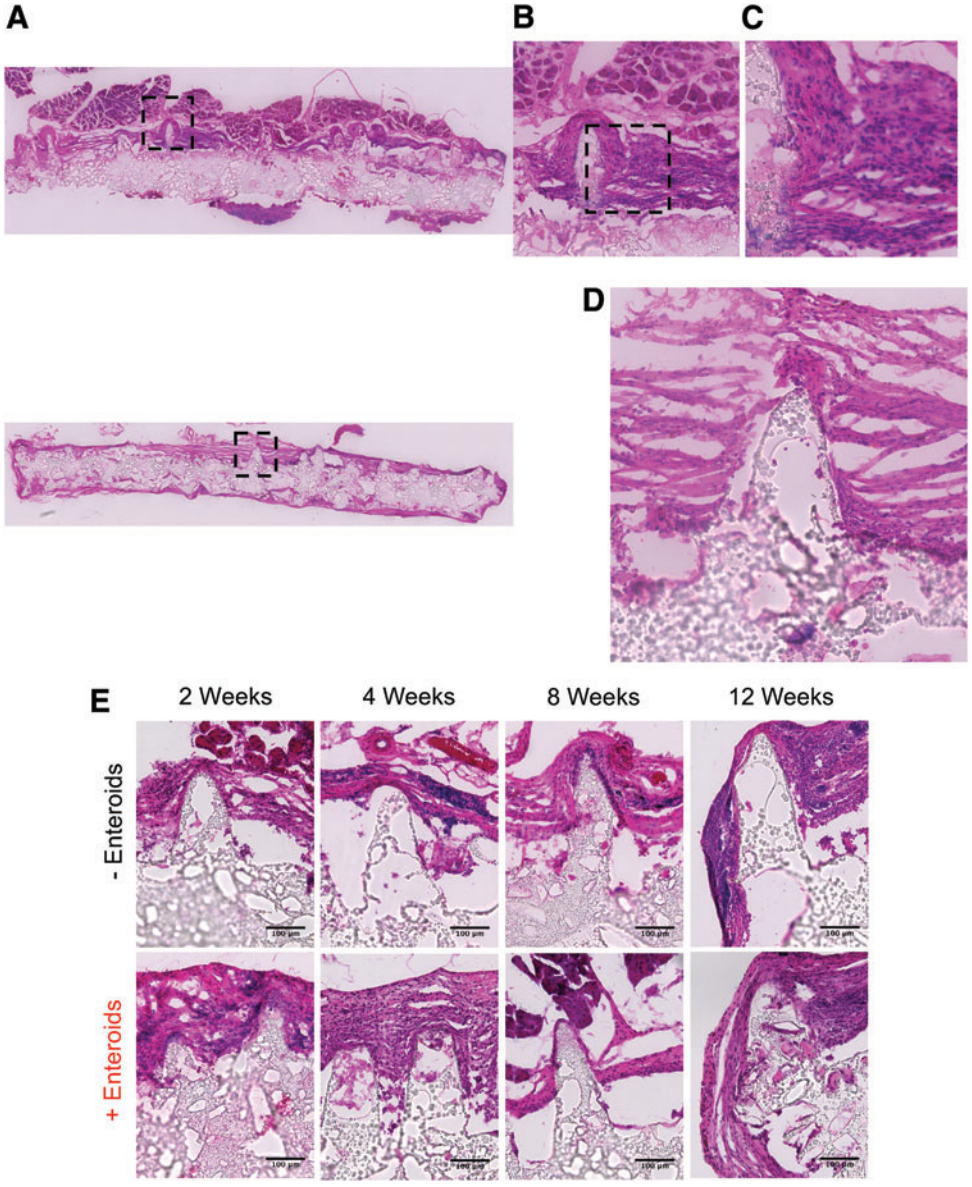

FIG. 7. Representative H&E staining of explanted scaffolds ($n = 6$ for each group at each time point, except for the +Enteroid group at 12 weeks ($n = 5$) and the −Enteroid group at 2 weeks ($n = 5$). **(A)** Tile scan views of an unseeded scaffold after 12 weeks of implantation (*top*) and seeded scaffold (*bottom*) at 200× magnification. The scaffold is surrounded by tissue with it covering the villi in this case. **(B)** A magnified view of the *black box* in **(A)** showing that the tissue consists of inflammatory cells. **(C)** A magnified view of the *black box* in **(B)** demonstrating that these cells appear to be primarily mononuclear in nature, likely representing macrophages or fibroblasts. **(D)** Magnified view of the seeded scaffold of the *black box* in **(A)**, *bottom image* showing that the tissue is primarily inflammatory. **(E)** Additional representative H&E images of unseeded and seeded scaffolds at each time point (scale bars = 100 μm). In general, they all demonstrate the presence of inflammation with some sections containing capillaries from the omentum (for example, the 4-week unseeded scaffold). H&E, hematoxylin and eosin. Color images are available online.

whether scaffolds were seeded or unseeded. In many cases, the scaffolds were completely surrounded with tissue and blood vessels could be seen near the surface of the scaffolds, presumably as part of the omentum. Interestingly, the scaffolds did not demonstrate significant tissue ingrowth, no architecturally detectable intestinal tissue was observed after implantation at any time points, nor was the tissue positive for intestinal epithelial cell markers (i.e., Lgr5, sucrase-isomaltase, Mucin 2, lysozyme, chromogranin A, and E-cadherin). We were also not able to identify any constitutively GFP-expressing cells even after staining with multiple GFP antibodies. We could not characterize with specificity the inflammatory cells present due to high background fluorescence of the scaffold, despite staining with numerous markers (CD45, F4/80, CD206, CD86, and myeloperoxidase), nor show evidence of mesenchymal cells or enteric nervous system when staining with the following markers: vimentin, α-smooth muscle actin, Sox10, glial fibrillary acidic protein, and P75. These findings suggest that implantation of the scaffolds was well tolerated by the mice and that the expected amount of inflammation occurred in response to implantation. More importantly, the scaffolds maintained their size and microarchitecture after implantation, even out to the long time point of 12 weeks. However, in this iteration of the scaffolds, we were not able to observe intestinal tissue formation. Taken in aggregate, we have developed intestinal villus scaffolds using PGS that mimic the biomechanical properties of native intestine and have a favorable degradation profile by maintaining their size and structure even after *in vivo* implantation

Discussion

We have described a scaffold designed specifically for intestinal tissue engineering that mimics the microarchitecture and has mechanical properties on the same scale as native intestine. The scaffolds have excellent retention of their architectural and mechanical properties during degradation both *in vitro* and *in vivo*. In addition, while we did not yet observe evidence of intestinal tissue formation upon implantation *in vivo*, the scaffolds had relatively good biocompatibility without severe inflammation. Thus, these scaffolds, after further optimization, may serve as excellent building blocks for future intestinal tissue engineering efforts.

To our knowledge, the use of the polymer PGS has not yet been reported for intestinal tissue engineering. PGS is an ideal polymer because it has tunable degradation rate and mechanical properties depending on the concentration of polymer solution used and the amount of crosslinking performed.[38] In addition, PGS degrades by surface degradation, which better enables the scaffold to maintain its structure as it degrades. Finally, PGS has been used extensively as a drug delivery polymer[39,40] and as such in future work, we can begin to incorporate growth factors and drugs to better encourage intestinal tissue formation and minimize inflammation. Because of these properties, PGS has been used in many fields of tissue engineering ranging from nerve, cardiac, vascular, and soft tissue.[41] This was our first attempt at using PGS in this novel scaffold fabrication technique and while efforts were made to optimize the properties of the scaffolds to match native intestine and promote tissue formation, we were not completely successful.

In vitro analysis demonstrated that the scaffolds had similar mechanical properties to native intestine, maintained their microarchitecture during *in vitro* degradation, had what appeared to be an appropriate mass loss during *in vitro* degradation, were cytocompatible with Caco-2 cells, and were able to accommodate seeded enteroids. It is noteworthy that after *in vivo* implantation, the scaffolds did not degrade as much as expected, suggesting they may provide structural support long term *in vivo*. While there was an expected amount of inflammation, there was no intestinal tissue formation observed and minimal tissue infiltration into the scaffold. These findings may have been the result of the lack of degradation of the scaffold. Because the scaffolds had such a slow degradation rate *in vivo*, it may have promoted ongoing, low-level inflammation and a foreign body response, which may have prevented the tissue formation we have previously seen with this scaffold structure using PLGA.[17] Based on our *in vitro* degradation studies, we would have expected the scaffolds to have lost at least 40–50% of their mass by 10 weeks and a concomitant decrease in size (given its known linear mass loss). It is possible that further optimization and varying the crosslinking amount will modify the degradation rate, and potentially leave behind a mold of native tissue that could achieve the goals of tissue replacement.

In addition to degradation rate, other important variables for tissue infiltration into scaffolds are pore size and porosity. In particular, pore sizes and porosity of at least 100 μm and 34.4%, respectively, are considered necessary for tissue infiltration after implantation.[42] The minimum pore size reported for angiogenesis is 30–40 μm, but a larger pore size of 160–270 μm improves angiogenesis and for vascularization of a construct, pore sizes as large as 300 μm are necessary.[42] In addition, pore size, porosity, and pore connectivity are known to affect cell proliferation and differentiation depending on cell type[42]; however, these effects have never been studied in intestinal epithelial cells or enteroids. These scaffolds were fabricated with dual pore size: 10 μm pores in the villus layer and 100–150 μm pores in the basal layer. The porosity of the scaffolds was 67%. The goal was to have the enteroids proliferate and spread out on the villus layer and for the basal layer to accommodate tissue infiltration and vasculogenesis. While it did appear that the enteroids were able to cover the scaffold and continue proliferation without infiltration past the villus architecture *in vitro*, the cells could not be detected *in vivo* and we observed quite poor tissue infiltration. This observation may reflect the effects of the current pore size and pore connectivity. Because the optimal pore size and porosity have not been studied for intestinal epithelium, these parameters will need to be determined for these particular scaffolds. In addition, while our pore sizes seemed adequate, on SEM, the pore connectivity was not ideal. Thus, we may need to incorporate a higher concentration of porogen particles during fabrication or change the method in which pores are created in the scaffolds.

In addition to optimizing porosity, these findings shed light on the ideal seeding method and time of *in vitro* culture before implantation. In our experiments, the enteroids were statically seeded in a small volume of media, which can result in inconsistent and nonuniform seeding. Thus, improved methods of seeding need to be explored and we are

currently in the process of designing a device to more consistently seed and maintain our constructs *in vitro*.[29] In this study, we chose 1 week of *in vitro* culture before implantation based on preliminary experiments comparing 1 week of culture to 2 weeks, which qualitatively showed nearly similar cell coverage at either time point (data not shown). The ideal time may be shorter than 1 week or longer than 2 weeks. Based on our results, looking at the microarchitectural changes of the seeded scaffolds *in vitro* (Fig. 2); however, it does not appear that longer time points in static culture would be beneficial because there were relatively few cells observed on SEM of the seeded scaffolds at 4 and 6 weeks. Developing a contained and efficient seeding device will simplify the process and improve consistency of seeding between experiments that will be critical in moving a technology such as artificial intestine toward clinical use. In addition, the development of a bioreactor that can improve cell coverage and potentially encourage differentiation should be explored. The ideal bioreactor would simulate peristalsis, have laminar fluid flow, incorporate electrical stimulation, and even allow for diffusion/absorption studies.

The use of PGS going forward is exciting as there is an opportunity to incorporate a variety of drugs or growth factors into the intestinal scaffolds to encourage the tissue type desired. In addition, due to our layered fabrication process, we can put different growth factors on the apical side compared to the basal side. For instance, we could include intestinal stem cell growth factors in the villi, such as Wnt3A, Noggin, and EGF, while placing anti-inflammatory and proangiogenic factors in the basal layer, such as steroids and vascular endothelial growth factor, respectively. In addition, we could create crypt spaces or pockets in the space between the villi where we concentrate the stem cell growth factors and better replicate the anatomic and physiologic scenario. Thus, as the cells proliferate upwards, they have less exposure to the growth factors and would be more likely to differentiate. Much more work will be needed to fabricate these scaffolds and characterize their drug release and efficacy, but the possibilities are exciting. While the ultimate goal for the development of these scaffolds is for use in artificial intestine, other possible applications exist. In particular, these constructs could serve as valuable tools for studying intestinal physiology and transport. This is especially true if they are successfully incorporated into an efficient, high-throughput seeding and bioreactor system, which has been done in other tissue types.[29,43–46]

While we believe that the PGS scaffolds are exciting, especially since we are approaching the mechanical properties of native intestine, this is not the first attempt at mimicking the native architecture of the intestine.[47–52] In addition, there are several limitations and shortcomings of this approach that deserve mention. First, while we were able to mimic the villus structure of the intestine, our scaffolds do not contain a crypt region. Other groups have been able to create a crypt-villus axis and with further modification of our fabrication process, this may be able to be included in future iterations. A second limitation was the inconsistent nature of the static seeding performed, which may have hindered the formation of intestinal tissue upon *in vivo* implantation. Others have developed and reported more sophisticated methods of seeding organoids onto scaffolds,[53,54] and we aim to incorporate these and develop our own techniques when moving forward (for instance by modifying the bioreactor already developed by Costello *et al.*[29]). Third, for these preliminary studies, we only evaluated how the PGS scaffolds performed and did not attempt to compare them to other, well-known and often used polymers such as poly(lactic) acid or PLGA. These comparisons should be made in future work. In addition, the scaffolds did exhibit inflammation, as expected, which was significant. While these constructs seem biocompatible based on our results, more work will be needed to reduce the inflammatory response. We postulate that the significant inflammatory response observed was, in part, due to the slower-than-expected degradation rate. Fourth, while the tensile properties of the scaffolds approached those of native intestine, we did not evaluate the ability of the scaffolds to withstand cyclic tensile loading; however, we did gain some understanding of their behavior under cyclic loading using compressive forces with rheometer measurements and stress-relaxation measurements. Understanding how the scaffolds will behave under cyclic loading, both tensile and compressive, will be important as the scaffolds will ultimately be exposed to cyclic peristaltic forces. Future work will include more stringent evaluations of both tensile and compressive cyclic loading. Fifth, in our degradation studies, we noted that some villi would break off of the scaffolds. We did not specifically account for this; however, on preliminary analysis of two of the scaffolds on which rheometer tests had been performed, a majority of the villi seemed to withstand testing, which involved 1–5 N of compressive preload and 10% shear strain (data not shown). Thus, it appears that the villi may tend to break over time with degradation or after *in vivo* implantation, although we certainly observed a large number of intact villi in scaffolds that had been implanted in the omentum. More work will be needed to ensure that as many villi as possible remain intact for long enough to allow tissue to form. Finally, given that this was an initial pilot and optimization study, we implanted the scaffolds into the omentum of mice since this is a well-described model and incubation system for developing artificial intestine.[13,55–58] The omentum, while a good model for evaluating tissue formation and biocompatibility, is limited by not exposing the implants to the gut flora or peristalsis, and the inability to evaluate absorption. Ultimately, we need to evaluate how these scaffolds will perform once implanted in continuity with small intestine. We have gained a small amount of experience with this in prior work when developing animal models for testing artificial intestine,[32] but much more work needs to be done to fully evaluate the PGS scaffolds in this setting.

In summary, we have now shown that PGS may serve as an excellent material for the formation of artificial intestine because it can be made to mimic the biomechanical properties of native intestine, has an excellent degradation profile both *in vitro* and *in vivo*, and is easy to handle and manipulate. Moreover, we were able to use it in the fabrication of intestinal villus scaffolds and the villus microarchitecture was maintained throughout our studies. Finally, the use of PGS for the development of artificial intestine is exciting because future work can include a variety of growth factors and/or drugs to further encourage intestinal tissue formation and vasculogenesis, while dampening inflammation.

Acknowledgments

The authors acknowledge the hard work and assistance of Barbara Smith, without whom the high-quality SEM images would not have been possible. The authors also acknowledge the other members of the Hackam lab, in particular Hongpeng Jia, Peng Lu, Thomas Prindle, Emilyn Banfield, Qinjie Zhou, Jungeun Sun, Diego Nino, Sanxia Wang, and Yukihiro Yamaguchi. Finally, the authors acknowledge the Timothy Phelps for the excellent illustration provided for the graphical abstract. M.R.L. received salary support during his contribution to this study under a National Institutes of Health National Institute of Diabetes and Digestive and Kidney Diseases T32 training grant (2T32DK007713-21). A.D.W. received salary support during his contribution to this study under a National Institutes of Health T32 training grant (5T32OD011089-42).

Data Availability

Raw and/or processed data will be made available upon request.

Disclosure Statement

No competing financial interests exist.

References

1. Spencer, A.U., Kovacevich, D., McKinney-Barnett, M., *et al.* Pediatric short-bowel syndrome: the cost of comprehensive care. Am J Clin Nutr **88,** 1552, 2008.
2. Nucci, A., Cartland Burns, R., Armah, T., *et al.* Interdisciplinary management of pediatric intestinal failure: a 10-year review of rehabilitation and transplantation. J Gastrointest Surg **12,** 429, 2008.
3. Modi, B.P., Langer, M., Ching, Y.A., *et al.* Improved survival in a multidisciplinary short bowel syndrome program. J Pediatr Surg **43,** 20, 2008.
4. Fitzgibbons, S.C., Ching, Y., Yu, D., *et al.* Mortality of necrotizing enterocolitis expressed by birth weight categories. J Pediatr Surg **44,** 1072, 2009.
5. Schalamon, J., Mayr, J.M., and Höllwarth, M.E. Mortality and economics in short bowel syndrome. Best Pract Res Clin Gastroenterol **17,** 931, 2003.
6. Ladd, M.R., Niño, D.F., March, J.C., Sodhi, C.P., and Hackam, D.J. Generation of an artificial intestine for the management of short bowel syndrome. Curr Opin Organ Transplant **21,** 178, 2016.
7. Martin, L.Y., Ladd, M.R., Werts, A., Sodhi, C.P., March, J.C., and Hackam, D.J. Tissue engineering for the treatment of short bowel syndrome in children. Pediatr Res **83,** 249, 2018.
8. Spencer, A.U., Neaga, A., West, B., *et al.* Pediatric short bowel syndrome: redefining predictors of success. Ann Surg **242,** 403, 2005.
9. Wales, P.W. Surgical therapy for short bowel syndrome. Pediatr Surg Int **20,** 647, 2004.
10. Oliveira, C., De Silva, N., and Wales, P.W. Five-year outcomes after serial transverse enteroplasty in children with short bowel syndrome. J Pediatr Surg **47,** 931, 2012.
11. Rege, A. The surgical approach to short bowel syndrome—autologous reconstruction versus transplantation. Viszeralmedizin **30,** 1, 2014.
12. Levin, D.E., and Grikscheit, T.C. Tissue-engineering of the gastrointestinal tract. Curr Opin Pediatr **24,** 365, 2012.
13. Vacanti, J.P., Morse, M.A., Saltzman, W.M., Domb, A.J., Perez-Atayde, A., and Langer, R. Selective cell transplantation using bioabsorbable artificial polymers as matrices. J Pediatr Surg **23,** 3, 1988.
14. Spurrier, R.G., Grant, C.N., Levin, D.E., Speer, A.L., and Grikscheit, T.C. Vitrification preserves murine and human donor cells for delayed generation of tissue-engineered small intestine. J Surg Res **186,** 646, 2014.
15. Levin, D.E., Barthel, E.R., Speer, A.L., *et al.* Human tissue-engineered small intestine forms from postnatal progenitor cells. J Pediatr Surg **48,** 129, 2013.
16. Grikscheit, T.C., Siddique, A., Ochoa, E.R., *et al.* Tissue-engineered small intestine improves recovery after massive small bowel resection. Ann Surg **240,** 748, 2004.
17. Shaffiey, S.A., Jia, H., Keane, T., *et al.* Intestinal stem cell growth and differentiation on a tubular scaffold with evaluation in small and large animals. Regen Med **11,** 45, 2016.
18. Boomer, L., Liu, Y., Mahler, N., *et al.* Scaffolding for challenging environments: materials selection for tissue engineered intestine. J Biomed Mater Res A **102,** 3795, 2014.
19. Gayer, C.P., and Basson, M.D. The effects of mechanical forces on intestinal physiology and pathology. Cell Signal **21,** 1237, 2009.
20. Guilak, F., Butler, D.L., Goldstein, S.A., and Baaijens, F.P.T. Biomechanics and mechanobiology in functional tissue engineering. J Biomech **47,** 1933, 2014.
21. Ingber, D.E., Wang, N., and Stamenović, D. Tensegrity, cellular biophysics, and the mechanics of living systems. Rep Prog Phys **77,** 1, 2014.
22. Ladd, M.R., Nin, D.F., and Hackam, D.J. Generation of an artificial intestine for the management of short bowel syndrome. Curr Opin Organ Transplant **21,** 178, 2016.
23. Costello, C.M., Hongpeng, J., Shaffiey, S., *et al.* Synthetic small intestinal scaffolds for improved studies of intestinal differentiation. Biotechnol Bioeng **111,** 1222, 2014.
24. Sato, T., Stange, D.E., Ferrante, M., *et al.* Long-term expansion of epithelial organoids from human colon, adenoma, adenocarcinoma, and Barrett's epithelium. Gastroenterology **141,** 1762, 2011.
25. Noel, G., Baetz, N.W., Staab, J.F., *et al.* A primary human macrophage-enteroid co-culture model to investigate mucosal gut physiology and host-pathogen interactions. Sci Rep **7,** 45270, 2017.
26. Sato, T., Vries, R.G., Snippert, H.J., *et al.* Single Lgr5 stem cells build crypt-villus structures in vitro without a mesenchymal niche. Nature **459,** 262, 2009.
27. Fujii, M., Matano, M., Nanki, K., and Sato, T. Efficient genetic engineering of human intestinal organoids using electroporation. Nat Protoc **10,** 1474, 2015.
28. Costello, C.M., Sorna, R.M., Goh, Y., Cengic, I., Jain, N.K., and March, J.C. 3-D intestinal scaffolds for evaluating the therapeutic potential of probiotics. Mol Pharmaceut **11,** 2030, 2014.
29. Costello, C.M., Phillipsen, M.B., Hartmanis, L.M., *et al.* Microscale bioreactors for in situ characterization of GI epithelial cell physiology. Sci Rep **7,** 1, 2017.
30. Sung, J.H., Yu, J., Luo, D., Shuler, M.L., and March, J.C. Microscale 3-D hydrogel scaffold for biomimetic gastrointestinal (GI) tract model. Lab Chip **11,** 389, 2011.

31. Tan, Q., Li, S., Ren, J., and Chen, C. Fabrication of porous scaffolds with a controllable microstructure and mechanical properties by porogen fusion technique. Int J Mol Sci **12,** 890, 2011.
32. Ladd, M.R., Martin, L.Y., Werts, A., *et al.* The development of newborn porcine models for evaluation of tissue engineered small intestine. Tissue Eng Part C Methods **24,** 331, 2018.
33. Wang, J., Wei, Y., Yi, H., *et al.* Cytocompatibility of a silk fibroin tubular scaffold. Mater Sci Eng C **34**, 429, 2014.
34. Schindelin, J., Arganda-Carreras, I., Frise, E., *et al.* Fiji: an open-source platform for biological-image analysis. Nat Methods **9,** 676, 2012
35. Ladd, M.R., Lee, S.J., Stitzel, J.D., Atala, A., and Yoo, J.J. Co-electrospun dual scaffolding system with potential for muscle-tendon junction tissue engineering. Biomaterials **32,** 1549, 2011.
36. Leaphart, C.L., Dai, S., Gribar, S.C., *et al.* Interferon-gamma inhibits enterocyte migration by reversibly displacing connexin43 from lipid rafts. Am J Physiol Gastrointest Liver Physiol **295,** G559, 2008.
37. Schuijers, J., Junker, J.P., Mokry, M., *et al.* Ascl2 acts as an R-spondin/wnt-responsive switch to control stemness in intestinal crypts. Cell Stem Cell **16,** 158, 2015.
38. Li, X., Hong, A.T.L., Naskar, N., and Chung, H.J. Criteria for quick and consistent synthesis of poly(glycerol sebacate) for tailored mechanical properties. Biomacromolecules **16,** 1525, 2015.
39. Wang, Y., Ameer, G.A., Sheppard, B.J., and Langer, R. A tough biodegradable elastomer. Nat Biotechnol **20,** 602, 2002.
40. Sun, Z.-J., Chen, C., Sun, M.-Z., *et al.* The application of poly (glycerol–sebacate) as biodegradable drug carrier. Biomaterials **30,** 5209, 2009.
41. Loh, X.J., Karim, A.A., and Owh, C. Poly(glycerol sebacate) biomaterial: synthesis and biomedical applications. J Mater Chem B **3,** 7641, 2015.
42. Loh, Q.L., and Choong, C. Three-dimensional scaffolds for tissue engineering applications: role of porosity and pore size. Tissue Eng Part B Rev **19,** 485, 2013.
43. Lovett, M., Rockwood, D., Baryshyan, A., and Kaplan, D.L. Simple modular bioreactors for tissue engineering: a system for characterization of oxygen gradients, human mesenchymal stem cell differentiation, and prevascularization. Tissue Eng Part C Methods **16,** 1565, 2010.
44. Saber, S., Zhang, A.Y., Ki, S.H., *et al.* Flexor tendon tissue engineering: bioreactor cyclic strain increases construct strength. Tissue Eng Part A **16,** 2085, 2010.
45. Moon, D.G., Christ, G., Stitzel, J.D., Atala, A., and Yoo, J.J. Cyclic mechanical preconditioning improves engineered muscle contraction. Tissue Eng Part A **14,** 473, 2008.
46. Yazdani, S.K., Tillman, B.W., Berry, J.L., Soker, S., and Geary, R.L. The fate of an endothelium layer after preconditioning. J Vasc Surg **51,** 174, 2010.
47. Pfluger, C.A., McMahon, B.J., Carrier, R.L., and Burkey, D.D. Precise, biomimetic replication of the multiscale structure of intestinal basement membrane using chemical vapor deposition. Tissue Eng Part A **19,** 649, 2013.
48. Wang, L., Murthy, S.K., Barabino, G.A., and Carrier, R.L. Synergic effects of crypt-like topography and ECM proteins on intestinal cell behavior in collagen based membranes. Biomaterials **31,** 7586, 2010.
49. Koppes, A.N., Kamath, M., Pfluger, C.A., *et al.* Complex, multi-scale small intestinal topography replicated in cellular growth substrates fabricated via chemical vapor deposition of parylene C. Biofabrication **8,** 035011, 2016.
50. Kim, S.H., Lee, J.W., Choi, I., Kim, Y.-C., Lee, J.B., and Sung, J.H. A microfluidic device with 3-D hydrogel villi scaffold to simulate intestinal absorption. J Nanosci Nanotechnol **13,** 7220, 2013.
51. Wang, Y., Gunasekara, D.B., Reed, M.I., *et al.* A microengineered collagen scaffold for generating a polarized crypt-villus architecture of human small intestinal epithelium. Biomaterials **128**, 44, 2017.
52. Kim, H.J., and Ingber, D.E. Gut-on-a-chip microenvironment induces human intestinal cells to undergo villus differentiation. Integr Biol **5,** 1130, 2013.
53. Kitano, K., Schwartz, D.M., Zhou, H., *et al.* Bioengineering of functional human induced pluripotent stem cell-derived intestinal grafts. Nat Commun **8,** 765, 2017.
54. Schwartz, D.M., Pehlivaner Kara, M.O., Goldstein, A., Ott, H.C., and Ekenseair, A. Spray delivery of intestinal organoids to reconstitute epithelium on decellularized native extracellular matrix. Tissue Eng Part C Methods **23,** 565, 2017.
55. Spurrier, R.G., Speer, A.L., Grant, C.N., Levin, D.E., and Grikscheit, T.C. Vitrification preserves murine and human donor cells for generation of tissue-engineered intestine. J Surg Res **190,** 399, 2014.
56. Spurrier, R.G., and Grikscheit, T.C. Tissue engineering the small intestine. Clin Gastroenterol Hepatol **11,** 354, 2013.
57. Chen, D.C., Avansino, J.R., Agopian, V.G., *et al.* Comparison of polyester scaffolds for bioengineered intestinal mucosa. Cells Tissues Organs **184,** 154, 2007.
58. Grikscheit, T.C., Ochoa, E.R., Ramsanahie, A., *et al.* Tissue-engineered large intestine resembles native colon with appropriate in vitro physiology and architecture. Ann Surg **238,** 35, 2003.

Address correspondence to:
David J. Hackam, MD, PhD
Division of Pediatric Surgery
The Johns Hopkins Children's Center
Johns Hopkins University
Room 7323
1800 Orleans Street
Baltimore, MD 21287

E-mail: dhackam1@jhmi.edu

Received: August 22, 2018
Accepted: December 5, 2018
Online Publication Date: August 21, 2019